This article has been accepted for publication in a future issue of this journal, but has not been fully edited. Content may change prior to final publication. Citation information: DOI 10.1109/TIV.2018.2873899, IEEE Transactions on Intelligent Vehicles

# Impact of Partial Penetrations of Connected and Automated Vehicles on Fuel Consumption and Traffic Flow

Jackeline Rios-Torres, *Member, IEEE,* *Andreas A. Malikopoulos, Senior Member, IEEE*

***Abstract*—This article addresses the problem of analyzing the effects of partial penetrations of optimally coordinated connected and automated vehicles (CAVs) on fuel consumption and travel time under low, medium, and heavy traffic volumes. We develop a microscopic simulation framework to enhance our understanding of the interactions between human-driven vehicles and CAVs in a merging on-ramp scenario. We show that fuel consumption is adversely affected for medium and high traffic while benefits are realized for travel time under the same traffic conditions. We also show that higher penetrations of CAVs contribute to more stable traffic patterns.**

***Index Terms*—Connected and automate vehicles (CAVs), merging highways, on-ramps, traffic analysis, cooperative merging control, car following, fundamental diagram, optimal control, energy implications.**

## I. Introduction

### A. Motivation

The goals of energy efficient mobility systems are to alleviate congestion, reduce energy use and emissions, and improve safety. The deep integration of technology in the transportation sector is providing fundamentally new methods to manage the flow of goods and people in our next generation transportation systems. Core disruptive technologies include vehicle connectivity, vehicle automation, and the notion of shared personalized transportation infrastructure enabled by mobility on demand systems. The overarching goal is to develop energy efficient mobility systems to connect communities and increase accessibility, without increasing the negative consequences of transportation (e.g., emissions, energy consumption, and congestion). We are currently witnessing an increasing integration of our energy and transportation, which, coupled with the human interactions, is giving rise to a new level of complexity [1] in transportation. As we move to increasingly complex transportation systems [2], new control approaches are needed to optimize the impact on system behavior of the interaction between vehicles at different traffic scenarios.

Intersections, merging roadways, speed reduction zones along with the drivers' responses to various disturbances are the primary sources of bottlenecks that contribute to traffic congestion and stop-and-go driving with significant implications in both, fuel consumption and traffic stability [3]–[7]. In 2015, congestion caused people in urban areas in US to spend 6.9 billion hours more on the road and to purchase an extra 3.1 billion gallons of fuel, resulting in a total cost estimated at $160 billion [8].

Connected and automated vehicles (CAVs) provide the most intriguing opportunity for enabling users to better monitor transportation network conditions and to improve traffic flow. CAVs can be controlled at different transportation segments, e.g., intersections, merging roadways, roundabouts, speed reduction zones and can assist drivers in making better operating decisions to improve safety and reduce pollution, fuel consumption, and travel delays [9].

### B. Literature Review

Several research efforts have considered approaches to achieve safe and efficient coordination of merging maneuvers with the intention to avoid severe stop-and-go driving. One of the very early efforts in this direction was proposed in 1969 by Athans [10]. Assuming a given merging sequence, Athans formulated the merging problem as a linear optimal regulator to control a single string of vehicles, with the aim of minimizing the speed errors that will affect the desired headway between each consecutive pair of vehicles. Later, a two-layer control scheme was proposed based on heuristic rules derived from observations of the non-linear system dynamics behavior [11]. Similar to Athans' approach, Awal et al. [12] developed an algorithm that starts by computing the optimal merging sequence to achieve reduced merging times for a group of vehicles that are closer to the merging point [10].

More recently, the problem of coordinating vehicles that are wirelessly connected to each other at merging roads was addressed [13]–[15]. A closed-form solution was developed aimed at optimizing the acceleration of each vehicle online, in terms of fuel consumption, while avoiding collision with

This manuscript has been authored by UT-Battelle, LLC, under Contract No. DE-AC05-00OR22725 with the US Department of Energy. The United States Government retains and the publisher, by accepting the article for publication, acknowledges that the United States Government retains a non-exclusive, paid-up, irrevocable, world-wide license to publish or reproduce the published form of this manuscript, or allow others to do so, for United States Government purposes.

This research was supported in part by the Laboratory Directed Research and Development Program of the Oak Ridge National Laboratory, Oak Ridge, TN 37831 USA, managed by UT-Battelle, LLC, for the US Department of Energy (DOE), and in part by UT-Battelle, LLC, through DOE contract DE-AC05-00OR22725 under DOE's SMART Mobility Initiative. This support is gratefully acknowledged.

Jackeline Rios-Torres is with the Energy and Transportation Science Division, Oak Ridge National Laboratory, Oak Ridge TN 37932 USA USA (phone: 865-946-1542; e-mail: riostorresj@ornl.gov).

Andreas A. Malikopoulos is with the Department of Mechanical Engineering, University of Delaware, DE 19716 USA (phone: 302-831-2889; e-mail: andreas@udel.edu).

This article has been accepted for publication in a future issue of this journal, but has not been fully edited. Content may change prior to final publication. Citation information: DOI 10.1109/TIV.2018.2873899, IEEE Transactions on Intelligent Vehicles

other vehicles at the merging region. The framework was later extended for mixed traffic (CAVs interacting with human-driven vehicles) to analyze the energy impact of different penetration rates of CAVs on the energy consumption [16]. In another research effort [17], a feedforward controller was proposed for vehicle coordination in merging maneuver with the aim to avoid collisions while imposing low communication requirements. Each vehicle will compute the required acceleration-deceleration profile to merge in a first-in-first-out (FIFO) sequence. Through simulations, the authors showed the efficacy of the algorithm to ensure a collision free merging. A freeway merging control algorithm was proposed in [18] for fully automated vehicles aimed at maximizing their average travel speed. The performance of the algorithm was analyzed under oversaturated traffic conditions and it was shown that for short safe headway times, the control strategy can reduce the queue formation on both, the main lane and the ramp. However, if the safe gap is chosen to be greater than $1.5$ sec, the queue formation is unavoidable.

There have been also some efforts reported in the literature towards enhancing our understanding of the effects of CAVs on traffic flow. A microscopic simulation model was presented in [19] to study the effects of an automated highway system on the average traffic speed. A mesoscopic and a macroscopic traffic flow models based on the dynamics of intelligent cruise control vehicles to describe the traffic flow characteristics was reported in [20]. The effectiveness of the efficiency of the models was demonstrated through simulations that revealed traffic flow differences with respect to the models representing manually driven vehicles. More recently, a framework was presented by [21] that uses different models and technology-related assumptions to simulate vehicles with distinct communication and level of automation capabilities.

### C. Contribution of the Paper

Most of the current research related to control and coordination of CAVs has been mainly focused on safety and travel time. Several studies have attempted to quantify the energy implications of proposed control and coordination strategies considering full penetration of CAVs. However, the implications of partial penetrations of CAVs on energy and travel time have been, to the best of our knowledge, an under-explored aspect. In our study we explore the impacts of our previously proposed optimal coordination framework for CAVs when there are interactions with human driven vehicles, i.e., for partial penetration rates of optimally coordinated CAVs, under different traffic conditions.

The contributions of this paper are: 1) the development of a simulation framework to capture the interaction of CAVs with human-driven vehicles under different traffic volumes in a merging on-ramp scenario, and 2) the analysis of the impact that different penetrations of CAVs have on fuel consumption, travel time and traffic flow.

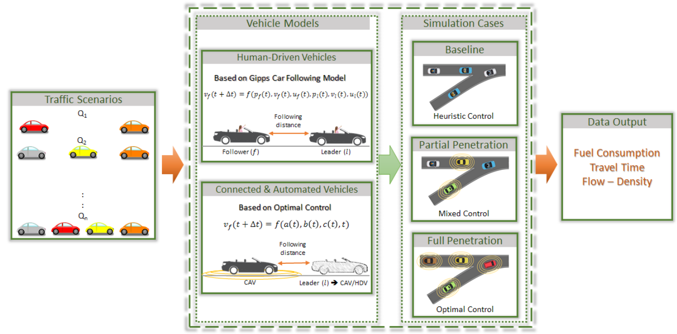


Fig. 1. Simulation framework for mixed traffic.

### D. Organization of the Paper

The remaining of the paper proceeds as follows. In Section II we introduce the simulation framework for mixed traffic environment. In Section III, we present the optimal control framework that can be used for CAVs. Finally, we provide simulation results in Section III and concluding remarks and discussion in Section IV.

## II. Simulation Framework

Our proposed simulation framework is illustrated in Fig. 1. To generate the data required to analyze of the implications of CAVs on different traffic conditions, we create different traffic scenarios by assuming a set of average traffic flows between 300 veh/h and 1400 veh/h. For the simulation of CAVs we use the optimal control framework proposed in [15] and for modeling the behavior of human drivers we adopt the Gipps car-following model [22]. We address three different cases: 1) a baseline case in which all the vehicles on the road are human-driven ($0\%$ CAV penetration), 2) a mixed traffic case in which the vehicles on the road can be either human-driven or different penetrations of CAVs, and 3) an ideal case in which all the vehicles on the road are CAVs ($100\%$ CAV penetration). We simulate all traffic scenarios for the aforementioned three cases and we analyze the results to quantify the impact on fuel consumption, travel time, and flow-density diagram. The details of these steps are described in the following subsections.

### A. Transportation Scenario

For this study, we considered a merging on-ramp (Fig. 2) consisting of a single lane main road and a single lane on-ramp. There is also a *merging zone* of length $S$, inside of which the vehicles complete the merging maneuver. For the cases where human-driven vehicles are involved, we consider that there is a *check zone* of length $D$, inside of which, the drivers attempt to estimate if there is a safe gap to merge; otherwise, they need to decelerate to avoid a lateral collision with the vehicles cruising on the main road. We consider that human-drivers will make decisions based on their perception of the surroundings and without using vehicle-to-vehicle (V2V) or vehicle-to-infrastructure (V2I) communication. For the cases where CAVs are involved in the same scenario, we use the

This article has been accepted for publication in a future issue of this journal, but has not been fully edited. Content may change prior to final publication. Citation information: DOI 10.1109/TIV.2018.2873899, IEEE Transactions on Intelligent Vehicles

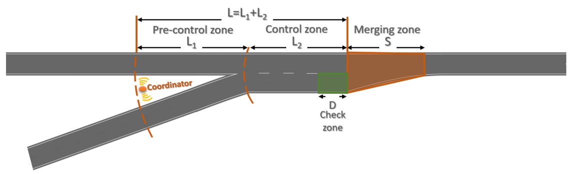


Fig. 2. Transportation scenario used for the study.

optimal control framework presented in [15]. In this framework, we consider that there is a *pre-control zone* of length $L_1$ and a *control zone* of length $L_2$. Once a CAV enters the pre-control zone, it computes its optimal acceleration-deceleration by using information from the preceding vehicle on a given FIFO queue. Without being restrictive in our analysis, we consider that $L_1 = L_2$.

### B. Traffic generation scenarios

To generate the different traffic scenarios, we use the shifted negative exponential distribution as proposed by the federal highway administration (FHWA) [23] aimed at deciding the inter-arrival time of the vehicles to the road section. According to this distribution, the vehicles will arrive at the entry of the pre-control zone following a given average vehicular flow as defined in equations (1) and (2)

$$h = (H - h_{min})[-ln(1-R)] + H - h_{min}, \tag{1}$$

$$H = 3600/Q_{avg}, \tag{2}$$

where $h$ is the headway time (s), $H$ is a desired mean headway time (s), $R$ is a random number between 0 and 1 and, $Q_{avg}$ is an average vehicular flow (veh/s).

### C. Optimal Control Framework

We adopt the optimization framework proposed in [15] for the scenario with CAVs. We consider a number of CAVs $N(t) \in \mathbb{N}$ in each lane, where $t \in \mathbb{R}^+$ is the time, entering the control zone (Fig. 2). Let $\mathcal{N}(t) = \{1, \ldots, N(t)\}$, be the FIFO queue inside the control zone. The dynamics of each vehicle $i \in \mathcal{N}(t)$ are represented by a state equation

$$\dot{x_i} = f(t, x_i, u_i), \qquad x_i(t_i^0) = x_i^0, \tag{3}$$

where $t \in \mathbb{R}^+$, $x_i(t)$, $u_i(t)$ are the state of the vehicle and control input, $t_i^0$ is the time that vehicle $i$ enters the control zone, and $x_i^0$ is the value of the initial state. For simplicity, we model each vehicle as a double integrator, e.g., $\dot{p}_i = v_i(t)$ and $\dot{v}_i = u_i(t)$, where $p_i(t) \in \mathcal{P}_i$, $v_i(t) \in \mathcal{V}_i$, and $u_i(t) \in \mathcal{U}_i$ denote the position, speed and acceleration/deceleration (control input) of each vehicle $i \in \mathcal{N}(t)$ inside the control zone. Let $x_i(t) = \begin{bmatrix} p_i(t) & v_i(t) \end{bmatrix}^T$ denote the state of each vehicle $i$, with initial value $x_i^0 = \begin{bmatrix} 0 & v_i^0 \end{bmatrix}^T$, taking values in the state space $\mathcal{X}_i = \mathcal{P}_i \times \mathcal{V}_i$.

For any initial state $(t_i^0, x_i^0)$ and every admissible control $u(t)$, the double integrator has a unique solution $x(t)$ on some interval $[t_i^0, t_i^m]$, where $t_i^m$ is the time that vehicle $i \in \mathcal{N}(t)$ enters the merging zone. In our framework we impose the following state and control constraints:

$$\begin{aligned} u_{i,min} \leqslant u_i(t) \leqslant u_{i,max}, \quad \text{and} \\ 0 \leqslant v_{min} \leqslant v_i(t) \leqslant v_{max}, \quad \forall t \in [t_i^0, t_i^m], \end{aligned} \tag{4}$$

where $u_{i,min}$, $u_{i,max}$ are the minimum and maximum control inputs (maximum deceleration/ acceleration) for each vehicle $i \in \mathcal{N}(t)$, and $v_{min}$, $v_{max}$ are the minimum and maximum speed limits respectively. For simplicity, in the rest of the paper we consider no vehicle diversity, and thus, we set $u_{i,min} = u_{min}$ and $u_{i,max} = u_{max}$.

For absence of any rear-end collision of two consecutive vehicles traveling on the same lane, the position of the preceding vehicle should be greater than or equal to the position of the following vehicle plus a safe distance $\delta(v_{ave}(t)) < S$, which is a function of the average speed of the vehicles inside the control zone. Thus, we impose the following rear-end safety constraint

$$s_i(t) = p_k(t) - p_i(t) \geqslant \delta(v_{ave}(t)), \ \forall t \in [t_i^0, t_i^m], \tag{5}$$

where $k$ denotes the vehicle that is physically located ahead of $i$ in the same lane, and $v_{ave}(t)$ is the average speed of the vehicles inside the control zone at time $t$.

*Definition 1:* For each vehicle $i \in \mathcal{N}(t)$, we define the set $\Gamma_i$ that includes only the positions along the lane where a lateral collision is possible, namely

$$\Gamma_i \triangleq \Big\{ p_i(t) \mid p_i(t) \in [L, L+S], \ \forall t \in [t_i^m, t_i^f] \Big\}. \tag{6}$$

where $t_i^f$ is the time that vehicle $i \in \mathcal{N}(t)$ exits the merging zone.

To avoid a lateral collision for any two vehicles $i, j \in \mathcal{N}(t)$ on different roads, the following constraint should hold

$$\Gamma_i \bigcap \Gamma_j = \varnothing, \forall t \in [t_i^m, t_i^f]. \tag{7}$$

The above constraint implies that only one vehicle at a time can be inside the merging zone. If the length of the merging zone is long, then this constraint might not be realistic since it results in dissipating space and capacity of the road. However, the constraint is not restrictive in the problem formulation and it can be modified appropriately as described in the following section.

In the modeling framework described above, we impose the following assumptions:

*Assumption 1:* The vehicles cruise inside the merging zone with the imposed speed limit, $v_{srz}$. This implies that for each vehicle $i$

$$t_i^f = t_i^m + \frac{S}{v_i(t_i^m)} = t_i^m + \frac{S}{v_{srz}}. \tag{8}$$

*Assumption 2:* Each vehicle $i$ has proximity sensors and can measure local information without errors or delays.

We briefly comment on the above assumptions. The first assumption is intended to enhance safety awareness, but it could be modified appropriately, if necessary. The second assumption may be a strong requirement to impose but it is

This article has been accepted for publication in a future issue of this journal, but has not been fully edited. Content may change prior to final publication. Citation information: DOI 10.1109/TIV.2018.2873899, IEEE Transactions on Intelligent Vehicles

relatively straightforward to extend our results in the case that it is relaxed, as long as the noise in the measurements and/or delays are bounded.

We consider the problem of deriving the optimal control input (acceleration/deceleration) of each CAV inside the pre-control and control zones (Fig. 2), under the hard safety constraint to avoid rear-end collision. By controlling the speed of the vehicles, the speed of queue built-up at the merging zone decreases, and thus the congestion recovery time is also reduced. The latter results in maximizing the throughput in the merging zone. Moreover, by optimizing the acceleration/deceleration of each vehicle, we minimize transient engine operation, thus we can have direct benefits in fuel consumption [24] and emissions since internal combustion engines are optimized over steady state operating points (constant torque and speed) [25], [26].

*1) Communication Structure of Connected and Automated Vehicles:*

*Definition 2:* Each CAV $i \in \mathcal{N}(t)$ belongs to at least one of the following two subsets of $\mathcal{N}(t)$ depending on its physical location inside the control zone: 1) $\mathcal{L}_i(t)$ contains all CAVs traveling on the same road and lane as vehicle $i$ and 2) $\mathcal{C}_i(t)$ contains all CAVs traveling on a different road from $i$ and can cause collision at the merging zone.

When a vehicle $i$ enters the control zone, it receives some information from the vehicle $i-1 \in \mathcal{N}(t)$ in the queue.

*Definition 3:* For each CAV $i$ entering the control zone, we define the *information set* $Y_i(t)$, which include all information without any errors or delays (Assumption 2) that each vehicle shares, as

$$Y_i(t) \triangleq \Big\{p_i(t), v_i(t), \mathcal{Q}, t_i^m\Big\}, \quad \forall t \in [t_i^0, t_i^m], \tag{9}$$

where $p_i(t), v_i(t)$ are the position and speed of CAV $i$ inside the control zone, $\mathcal{Q} \in \{1,2\}$ is the subset assigned to CAV $i$ by the coordinator, and $t_i^m$, is the time targeted for CAV $i$ to enter the merging zone, whose evaluation is discussed next.

A "coordinator" handles the information between the vehicles as follows. When a CAV reaches the pre-control zone at some instant $t$, the coordinator assigns a *unique identity* to each vehicle $i \in \mathcal{N}(t)$, which is a pair $(i,j)$, where $i = N(t)+1$ is an integer representing the location of the vehicle in a FIFO queue $\mathcal{N}(t)$ and $j \in \{1,2\}$ is an integer based on a one-to-one mapping from $\mathcal{L}_i(t)$ and $\mathcal{C}_i(t)$ onto $\{1,2\}$. If the vehicles enter the control zone at the same time with the same initial speed, then the coordinator selects randomly their position in the queue.

The time $t_i^m$ that the vehicle $i$ will be entering the merging zone is restricted by the imposing rear-end and lateral collision constraints. Therefore, to ensure that (5) and (7) are satisfied at $t_i^m$ we impose the following conditions which depend on the subset that the vehicle $i-1$ belongs to:

If vehicle $i-1 \in \mathcal{L}_i(t)$

$$t_i^m = \max\left\{ \min\left\{t_{i-1}^m + \frac{\delta(v_{ave}(t))}{v_{i-1}(t_{i-1}^m)}, \frac{L}{v_{min}}\right\}, \frac{L}{v_i(t_i^0)}, \frac{L}{v_{max}}\right\}, \tag{10}$$

if vehicle $i-1 \in \mathcal{C}_i(t)$

$$t_i^m = \max\left\{ \min\left\{t_{i-1}^m + \frac{S}{v_{i-1}(t_{i-1}^m)}, \frac{L}{v_{min}}\right\}, \frac{L}{v_i(t_i^0)}, \frac{L}{v_{max}}\right\}, \tag{11}$$

where $v_{i-1}(t_{i-1}^m)$ is the speed of the vehicle $i-1$ at the time $t_{i-1}^m$ that enters the merging zone, and it is equal to the speed, $v_{srz}$, imposed inside the merging zone (Assumption 1). The conditions (10) and (11) ensures that the time $t_i^m$ each vehicle $i$ will be entering the merging zone is feasible and can be attained based on the imposed speed limits inside the control zone. In addition, for low traffic flow where vehicle $i-1$ and $i$ might be located far away from each other, there is no compelling reason for vehicle $i$ to accelerate within the control zone to have a distance $\delta(v_{ave}(t))$ from vehicle $i-1$, if $i-1 \in \mathcal{L}_i(t)$, or a distance $S$ if $i-1 \in \mathcal{L}_i(t)$, at the time $t_i^m$ that vehicle $i$ enters the merging zone. Therefore, in such cases vehicle $i$ can keep cruising within the control zone with the initial speed $v_i(t_i^0)$ that entered the control zone at $t_i^0$. The recursion is initialized when the first vehicle enters the control zone, i.e., it is assigned $i=1$. In this case, $t_1^m$ can be externally assigned as the desired exit time of this vehicle whose behavior is unconstrained. Thus the time $t_1^m$ is fixed and available through $Y_1(t)$. The second vehicle will access $Y_1(t)$ to compute the times $t_2^m$. The third vehicle will access $Y_2(t)$ and the communication process will continue with the same fashion until the vehicle $N(t)$ in the queue access the $Y_{N(t)-1}(t)$.

*2) Optimal Control Problem Formulation for Connected and Automated Vehicles:* Since the coordinator is not involved in any decision on the vehicle coordination framework we can formulate $N(t)$ sequential decentralized control problems that may be solved on line:

$$\min_{u_i} \frac{1}{2}\int_{t_i^0}^{t_i^m} u_i^2(t)\ dt, \tag{12}$$
$$\text{subject to : (3) and (4)},$$

with initial and final conditions: $p_i(t_i^0) = 0$, $p_i(t_i^m) = L$, $t_i^0$, $v_i(t_i^0)$, $t_i^m$, and $v_i(t_i^m) = v_{srz}$. In the problem formulation above, we have omitted the rear end (5) and lateral (7) collision safety constraints. As mentioned earlier, (7) is implicitly handled by the selection of $t_i^m$ in (11). Eq. (5) is omitted because it has been shown [27] that the solution of (12) guarantees that this constraint holds throughout $[t_i^0, t_i^f]$. Thus, (12) is a simpler problem to solve on line.

For the analytical solution and real-time implementation of the control problem (12), we apply Hamiltonian analysis. In our analysis, we consider that when the vehicles enter the control zone, none of the constraints are active. To address this problem, the constrained and unconstrained arcs need to be pieced together to satisfy the Euler-Lagrange equations

This article has been accepted for publication in a future issue of this journal, but has not been fully edited. Content may change prior to final publication. Citation information: DOI 10.1109/TIV.2018.2873899, IEEE Transactions on Intelligent Vehicles

and necessary condition of optimality. The analytical solution of (12) without considering state and control constraints was presented in earlier papers [13]–[15] for coordinating in real time CAVs at highway on-ramps and [28] at two adjacent intersections. When the state and control constraints are not active, the optimal control input (acceleration/deceleration) as a function of time is given by

$$u_i^*(t) = a_i t + b_i., \tag{13}$$

and the optimal speed and position for each vehicle are

$$v_i^*(t) = \frac{1}{2}a_i t^2 + b_i t + c_i \tag{14}$$

$$p_i^*(t) = \frac{1}{6}a_i t^3 + \frac{1}{2}b_i t^2 + c_i t + d_i, \tag{15}$$

where $a_i$, $b_i$, $c_i$ and $d_i$ are constants of integration. These constants can be computed by using the initial and final conditions. Since we seek to derive the optimal control (13) in real time, we can designate initial values $p_i(t_i^0)$ and $v_i(t_i^0)$, and initial time, $t_i^0$, to be the current values of the states $p_i(t)$ and $v_i(t)$ and time $t$, where $t_i^0 \le t \le t_i^m$. Similar results to (13)-(15) can be obtained when the state and control constraints become active [27].

### D. Human-driven vehicles model

The Gipps car following model is used to represent the drivers' behavior. It aims to keep a safe following distance from the leader vehicle or to travel at a desired speed in free traffic [22], [29]–[31]. The speed $v_f$ of the follower vehicle is computed as

$$v_f(t+\tau) = \min\{v_{f,acc}(t+\tau), v_{f,dec}(t+\tau)\}, \tag{16}$$

$$v_{f,acc}(t+\tau) = v_f(t) + 2.5u_{f,max}\tau \cdot \left(1 - \frac{v_f(t)}{v_{f,max}}\right) \cdot \sqrt{0.025 + \frac{v_f(t)}{v_{f,max}}}, \tag{17}$$

$$v_{f,dec}(t+\tau) = u_{f,min}\tau + \left(u_{f,min}^2\tau^2 - u_{f,min}\left(2(p_l(t) - p_f(t) - (L_{veh} + f_d)) - v_f(t)\tau - \frac{v_f(t)}{\hat{u}_{l,min}}\right)\right)^{1/2}, \tag{18}$$

where the subscripts $f$, $l$ identify the follower and the leader respectively, $\tau$ represents both the driver's reaction time and sample time of the simulation, $v_{acc}$ is the speed when the vehicle is not constrained by the traffic, $v_{dec}$ is the speed when the vehicle is constrained by a leader in front, $p$ is the vehicle position, $v$ is the vehicle speed, $v_{f,max}$ is the maximum desired speed, $u_{f,max}$ is the maximum desired acceleration, $u_{f,min}$ is the highest allowed braking value, $\hat{u}_{l,min}$ is the follower's estimation of the leader highest braking value, $L_{veh}$ is the vehicle length, and $f_d$ is the desired headway distance when the vehicles are at stop. To ensure a collision-free trip, the follower's highest desired braking must be greater than or equal to the leader's highest braking value, namely

$$u_{f,min} \ge \hat{u}_{l,min}, \tag{19}$$

We consider the merging roadways in Fig. 2 and assume that all the vehicles behave according to the Gipps car-following model [22]. Therefore, the vehicles do not receive information from nearby vehicles nor the infrastructure. They use estimations of their leading vehicle behavior to decide on the safe speed at each sample time. Several studies have shown that this model can represent driver behaviors with acceptable accuracy, and it is used in traffic simulation software like AIMSUN [30], [31].

In the merging scenario we consider here, each vehicle traveling on the main road deems the preceding vehicle as its leader and follows the speed designated by the Gipps model until it reaches the merging zone. Once the vehicle enters the merging zone, then it evaluates whether it has a new leader to follow. In the case that a new leader is identified, the vehicle will adjust its speed to keep a safe distance and avoid a rear-end collision with its new leader.

Similarly, each vehicle traveling on the secondary road will consider its preceding vehicle on the same road as its leader until it reaches a distance $D$ from the merging zone and the leader has merged into the main road. Then, if a safe gap to merge into the main road is available, the vehicle will adjust its speed to merge and continue following the new leader while maintaining a safe distance. If there is not a gap available, the vehicle will come to a stop before the merging zone and wait for the next available gap. Once a safe gap is identified, the vehicle will accelerate to merge and will behave according to the Gipps car-following model again.

## III. Simulation Framework

We consider the traffic scenario illustrated in Fig. (2), where the pre-control and control zones are of length $L_1 = L_2 = 200$ $m$, and the merging and check zones are of length $S = D = 30$ $m$. We assume that the human drivers attempt to reach and maintain a desired speed $v_{des} = 13.41$ $m/s$ and will use the check zone to evaluate the merging conditions and to decide whether to accelerate to merge or decelerate and wait for the next safe gap on the main road. We also assume the CAVs support V2V and V2I communication and attempt to reach and maintain a desired speed $v_{des} = 13.41$ $m/s$ before entering and after leaving the merging zone. Note that these values are not restrictive and can be modified accordingly.

We seek to study the impact of the gradual penetration of CAVs on fuel consumption, travel time and traffic flow under different traffic conditions. To accomplish this goal, we first generate sets of entry volumes varying from 300 $veh/h$ to 1400 $veh/h$ for a total of 300 vehicles. To analyze the effects in fuel consumption, we use the vehicles' speed and acceleration/deceleration trajectories from the moment the vehicles enter the pre-control zone until they exit the merging zone. Fuel consumption is computed with respect

This article has been accepted for publication in a future issue of this journal, but has not been fully edited. Content may change prior to final publication. Citation information: DOI 10.1109/TIV.2018.2873899, IEEE Transactions on Intelligent Vehicles

to speed and acceleration/deceleration using the polynomial meta-model proposed in [32]. The time that each vehicle takes to travel from the beginning of the pre-control zone to the end of the merging zone is also recorded in order to compute the total travel time. To analyze the effects of gradual penetrations of CAVs on the traffic flow, we aggregated data related to traffic (i.e., travel time, traffic volume, average speed and queue) every 30 $sec$ and used it to plot the traffic flow as a function of traffic density.

We simulate each set of entry volumes for the three cases discussed in the following subsections. To account for the stochastic nature of traffic and driver behaviors, we repeate the complete set of simulations, i.e., different entry volumes for the three cases, five times. The final measures of travel time and fuel consumption correspond to the average value for the five runs.

### A. Case 1: No CAVs Penetration

We consider that all the vehicles entering the traffic segment behave according to the Gipps car following model. This case is the baseline scenario.

### B. Case 2: Full CAVs Penetration

We consider that all the vehicles on the traffic segment are CAVs computing their own optimal path by using local information received from other vehicles and the infrastructure via V2V or V2I.

### C. Case 3: Partial CAVs Penetration

Since we seek to analyze the impacts of mixed traffic, we combine the Gipps car following model and the optimal control framework of CAVs. To explore the effects of gradual penetration of CAVs, we simulate seven penetration rates ranging from $10\%$ to $80\%$ for each set of entry volumes. From the total number of vehicles, we select randomly which vehicle will be human-driven and which one will be a CAV.

## IV. Simulation Results

For low traffic volume, fuel consumption decreases as the penetration of CAVs increases (Fig. 3). At very low traffic flows (300 $veh/h$ to 500 $veh/h$) the travel time decreases significantly only for full CAVs penetration (Fig. 6). At $0\%$ penetration (case 1) the drivers on the ramp have to yield to the vehicles on the main road until a safe gap is available to merge. This eventually creates a queue on the ramp with frequent stop-and-go driving patterns and, as a consequence, fuel consumption is increased. In contrast, for full and partial penetration rates (cases 2 and 3) there are significant savings in fuel consumption as the vehicles cooperate to merge smoothly without stopping on the ramp. In particular, for full CAVs penetration the savings can vary from $40\%$ to $55\%$. Note that the travel time increases slightly for some penetration rates of CAVs (Fig. 6) since some of them are limited by the human-driven vehicles which have to stop on the ramp and wait for a gap to merge.

For medium and high traffic volumes, total fuel consumption is reduced only at $100\%$ penetration of CAVs (Fig. 4 and Fig. 5), while significant benefits are realized in travel time only when there are more than $40\%$ CAVs on the road (Fig. 7 and Fig. 8). At $100\%$ penetration of CAVs, total fuel consumption decreases by $16\%$ to about $60\%$ and the travel time between $40\%$ and $67\%$ . Notably, the highest benefit in travel time (67%) and fuel savings ($63\%$) are achieved at medium traffic conditions as CAVs are able to communicate with each other and follow the optimal control without the disturbances induced by human-drivers. Furthermore, in moderate traffic they will be driving closer to each other but will still have more freedom (and headways) to perform the optimal acceleration/deceleration patterns computed by the optimal control as opposed to the heavy traffic case. Thus the higher fuel saving percentages are achieved for moderate traffic. In mixed traffic, the CAVs following a human-driven vehicle are constrained by the random acceleration/deceleration choices of the driver and the lack of communication, so they will need to rely on their own estimations (through sensors) to ensure a collision-free trajectory. This implies that the CAVs will be adversely affected by the stop-and-go driving of the human-driven vehicles when attempting to merge and will be required to perform harder acceleration/deceleration maneuvers to ensure safety, resulting in consuming more fuel. This becomes particularly critical for the total travel time at low CAVs penetration as a considerable number of human-driven vehicles will be stoping to find a gap to merge and the CAVs will have to decelerate/stop more often affecting the traffic behind them. As the CAVs penetration rate goes over $50\%$, there are more CAVs communicating with each other and able to follow the optimal control inputs, and thus, decreasing the overall travel time. Notably, as the traffic starts increasing, CAVs are more constrained to follow the optimal trajectories due the lack of communication with the human-driven vehicles and the inaccurate prediction of their future behavior. Thus, the traffic becomes increasingly unstable and even with 80% CAVs penetration, the unpredicted behavior of human drivers who could still have random acceleration/deceleration choices, and even stop-and-go driving when attempting to merge, will affect the upstream traffic producing a negative impact on the fuel consumption. However, it is still evident that, as the number of CAVs on the road exceeds the number of human-driven vehicles, their optimal operation has a positive influence on the the overall traffic.

Summarizing, under low traffic volumes, fuel savings are realized for all CAVs penetration rates. At very low demands the travel time remain almost constant, but as the demand starts increasing travel time savings are achieved. For moderate traffic volumes, fuel savings are realized only in the full penetration case while travel time savings are still achieved in most cases. For higher traffic volumes, fuel savings are again realized only in the full penetration case, and the travel time will be significantly reduced only when at least 40% of the vehicles on the road are CAVs being optimally coordinated.

To analyze how the traffic evolves as CAVs gradually penetrates in the scenario under analysis, we used the aggregated traffic data to plot the traffic flow versus density for

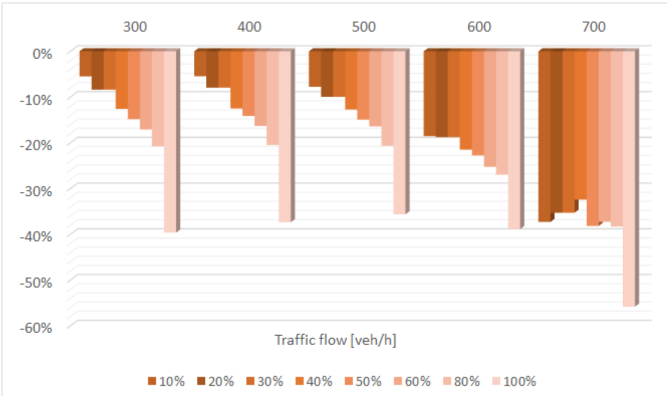


Fig. 3. Fuel savings with respect to the baseline scenario for different penetrations of CAVs under low average traffic demand.

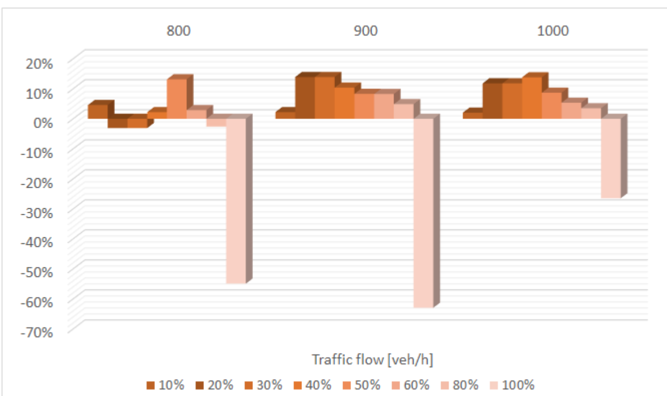


Fig. 4. Fuel savings with respect to the baseline scenario for different penetrations of CAVs under medium average traffic demand.

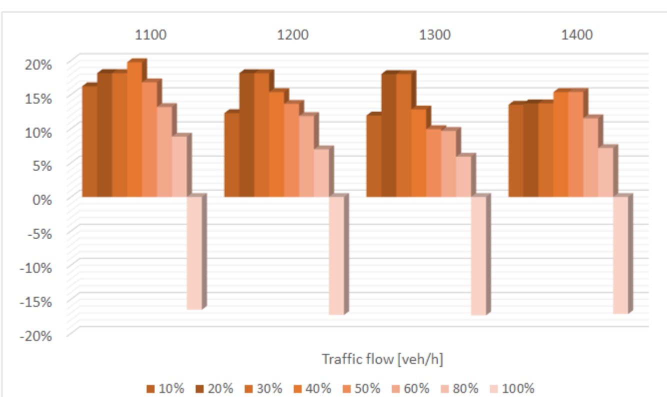


Fig. 5. Fuel savings with respect to the baseline scenario for different penetrations of CAVs under high average traffic demand.

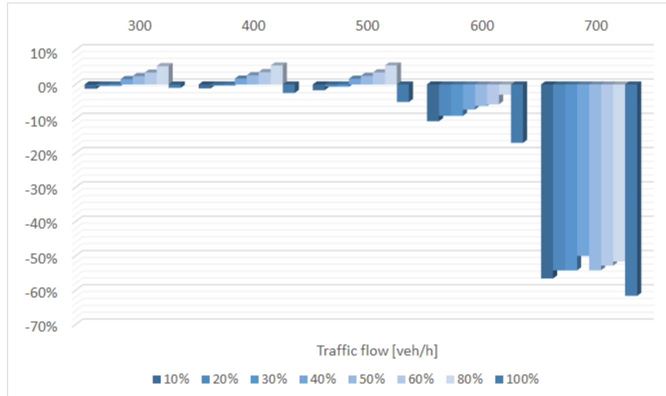


Fig. 6. Travel time savings with respect to the baseline scenario for different penetrations of CAVs under low average traffic demand.

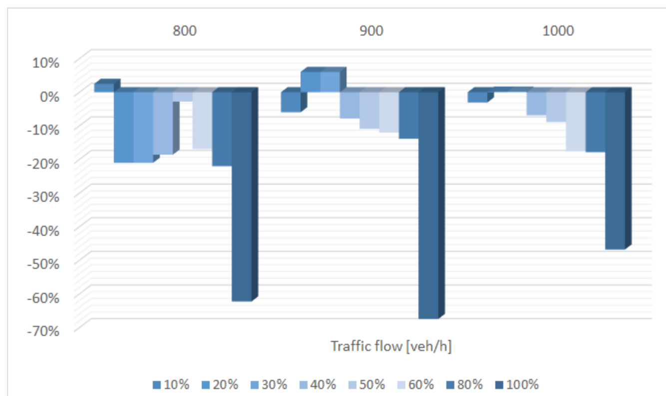


Fig. 7. Travel time savings with respect to the baseline scenario for different penetrations of CAVs under medium average traffic demand.

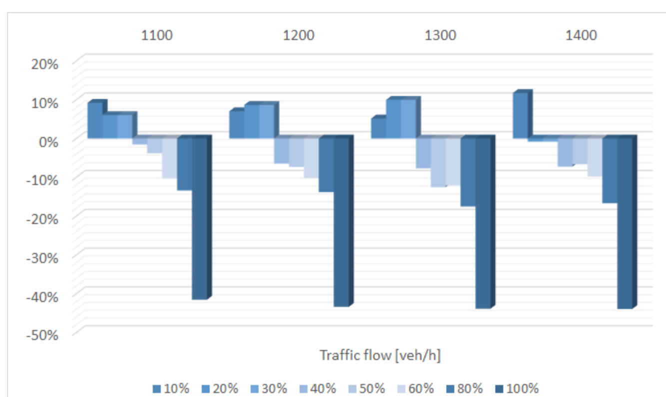


Fig. 8. Travel time savings with respect to the baseline scenario for different penetrations of CAVs under high average traffic demand.

different CAVs penetration values, i.e., $0\%$, $10\%$, $20\%$, $30\%$, $40\%$, $50\%$, $60\%$, $80\%$, and $100\%$. Figure 9 illustrates the flow-density plots for low CAVs penetrations ($0\%$, $10\%$ and $20\%$). In the baseline case ($0\%$), the traffic flow is scattered and mostly concentrated below $1500\ veh/h$ while the road utilization remains at low values. At low CAVs penetrations, i.e., $10\%$ and $20\%$, the data points representing congested traffic become even more scattered while the road utilization starts increasing. The increased instability of the traffic flow at low penetrations is attributed to the fact that CAVs are not able to accurately estimate the behavior of human-driven vehicles and need to constantly self-adjust their controls, or over-write their computed optimal inputs, to ensure a collision-free trip. This implies that CAVs will be more prone to sudden decelerations that will be reflected in the downstream traffic.

The flow-density plots for medium CAVs penetrations ($30\%$, $40\%$ and $50\%$) are illustrated in Fig. 10. Even though the traffic is still increasingly unstable at medium penetration values, it is possible to observe that the low traffic flow data points start moving upward, i.e., dots representing traffic flows below 500 veh/h start moving up the plot as the CAVs penetration rate increases. It is also observed an increasing trend for the traffic density, i.e., the road utilization increases.

Figure 11 illustrates the flow-density plots for higher CAVs penetration rates ($60\%$, $80\%$ and $100\%$). At higher penetrations ($60\%$ and $80\%$) the data points are still scattered on the plot. However, the traffic becomes more stable and the data points start concentrating at higher traffic flows ($> 500\ veh/h$) and higher densities ($> 100\ veh/km$) given that more CAVs are on the road communicating with each other and coordinating to merge. At full penetration ($100\%$), and for average traffic values less than $1500\ veh/h$ the traffic flows freely, i.e., there is not congestion. As the traffic start reaching the road capacity, some congestion can still occur (at high traffic flows and densities), but in general the flow-density diagram shows a significant reduction in the traffic flow variations compared to the mixed traffic conditions.

## V. Concluding Remarks and Discussion

Given the limited number of CAVs that have already been deployed on the roads, there is not enough data available that can be used to make conclusive statements on the implications of CAVs on fuel consumption and traffic conditions. Therefore, it is important to identify alternatives to start analyzing the operation of CAVs and their influence on traffic efficiency and fuel consumption, particularly when operating in mixed environments, i.e., interacting with human-driven vehicles.

In this paper, we developed a simulation framework to analyze the impact of CAVs on fuel consumption, travel time and traffic flow in a merging on-ramp scenario under different traffic volumes and penetration rates. The CAVs are optimally coordinated with the aim to reduce fuel consumption while the human-driven vehicles behave according to the Gipps car following model. For the mixed traffic cases and to allow safe operation of CAVs under the constraint of high traffic flows, we considered that the optimal control inputs are overwritten if a threshold in the distance with the leader vehicle is violated.

The simulation results revealed that the benefits in fuel consumption are realized under the following conditions: (1) $100\%$ penetration of CAVs under any traffic volume and (2) in mixed traffic only when the traffic volume is low. In contrast, the benefits in travel time are realized under the following conditions (1) all the vehicles are CAVs traveling under medium and high traffic flows and (2) in mixed traffic under medium and high traffic flows only if there are more than 50% CAVs on the road.

In the case of travel time, for lower CAVs penetration, the low number of CAVs on the roads are adversely affected by the "random" human driving patterns. Finally, by comparing the flow-density diagrams for different CAVs penetration, we observed that as the number of CAVs on the road communicating and coordinating their operation increases the traffic patterns become more stable.

Ongoing work is exploring whether it is possible to account for human-behavior when optimizing the operation of CAVs so that in addition to benefits in travel time, benefits in fuel consumption can also be realized under partial penetration scenarios. Future work should analyze the effects of gradual CAVs penetration for different traffic scenarios and whether CAVs can be used to have indirect control on human-drivers with the aim to achieve reduced fuel consumption and more stable traffic patterns in mixed traffic conditions.

## VI. Acknowledgments

This manuscript has been authored by UT-Battelle, LLC, under Contract No. DE-AC05-00OR22725 with the U.S. Department of Energy (DOE). The United States Government retains and the publisher, by accepting the article for publication, acknowledges that the United States Government retains a nonexclusive, paid-up, irrevocable, world-wide license to publish or reproduce the published form of this manuscript, or allow others to do so, for United States Government purposes. This report and the work described were sponsored by the U.S. Department of Energy (DOE) Vehicle Technologies Office (VTO) under the Systems and Modeling for Accelerated Research in Transportation (SMART) Mobility Laboratory Consortium, an initiative of the Energy Efficient Mobility Systems (EEMS) Program. The authors acknowledge Erik Rask of Argonne National Laboratory for leading the CAVs Pillar of the SMART Mobility Laboratory Consortium. The following DOE Office of Energy Efficiency and Renewable Energy (EERE) managers played important roles in establishing the project concept, advancing implementation, and providing ongoing guidance: David Anderson. Additional support was received from the Laboratory Directed Research and Development Program of the Oak Ridge National Laboratory, Oak Ridge, TN 37831 USA, managed by UT-Battelle, LLC, for the DOE. These supports are gratefully acknowledged.

This article has been accepted for publication in a future issue of this journal, but has not been fully edited. Content may change prior to final publication. Citation information: DOI 10.1109/TIV.2018.2873899, IEEE Transactions on Intelligent Vehicles

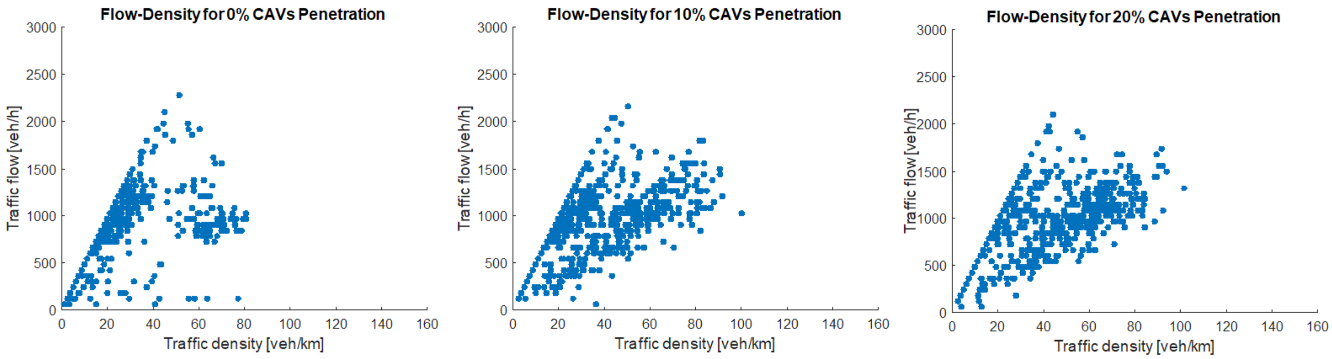


Fig. 9. Traffic flow vs traffic density for low CAVs penetration rates (0%, 10% and 20%).

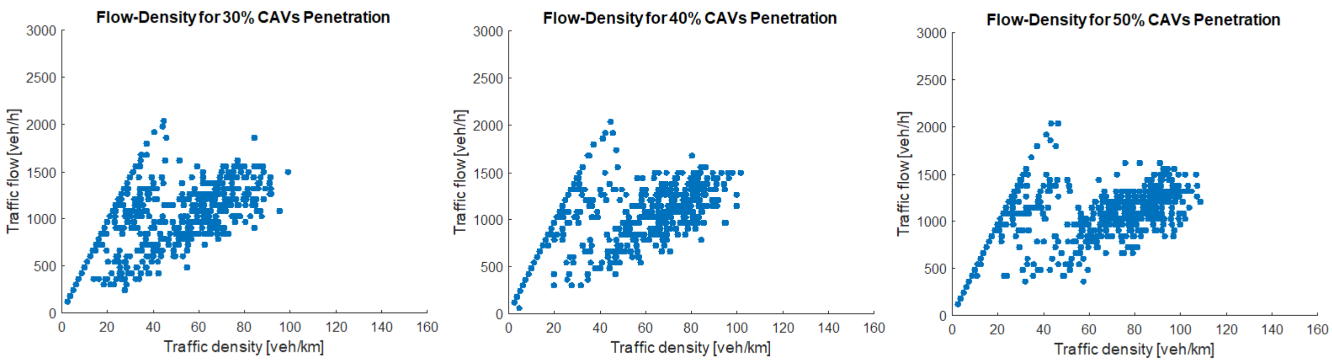


Fig. 10. Traffic flow vs traffic density for medium CAVs penetration rates (30%, 40% and 50%).

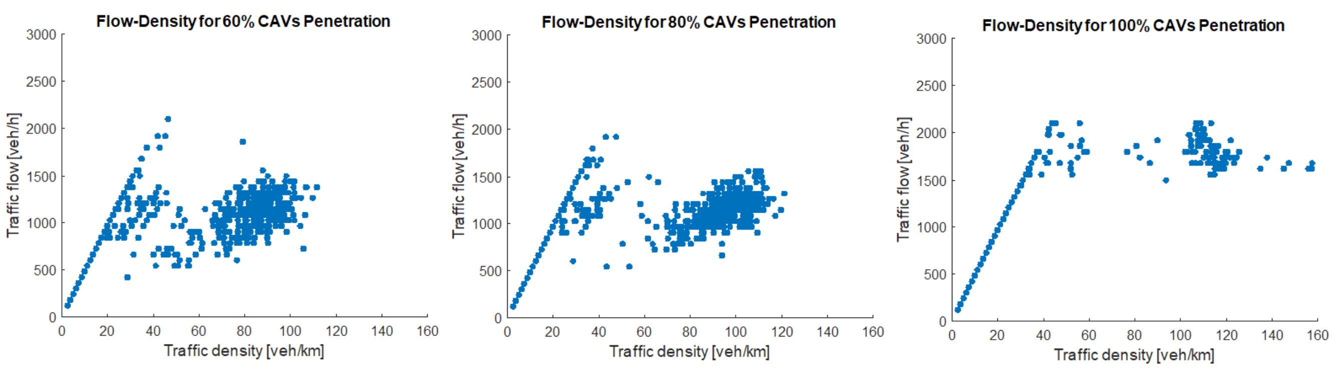


Fig. 11. Traffic flow vs traffic density for high CAVs penetration rates (60%, 80% and 100%).

## REFERENCES

[1] A. A. Malikopoulos, "Centralized stochastic optimal control of complex systems," in *Proceedings of the 2015 European Control Conference*, 2015, pp. 721–726.

[2] ——, "A duality framework for stochastic optimal control of complex systems," *IEEE Transactions on Automatic Control*, vol. 61, no. 10, pp. 2756–2765, 2016.

[3] V. L. Knoop, H. J. Van Zuylen, and S. P. Hoogendoorn, "Microscopic Traffic Behaviour near Accidents," in *18th International Symposium of Transportation and Traffic Theory*. Springer, New York, 2009.

[4] R. Margiotta and D. Snyder, "An agency guide on how to establish localized congestion mitigation programs," U.S. Department of Transportation. Federal Highway Administration, Tech. Rep., 2011.

[5] A. A. Malikopoulos and J. P. Aguilar, "An Optimization Framework for Driver Feedback Systems," *IEEE Transactions on Intelligent Transportation Systems*, vol. 14, no. 2, pp. 955–964, 2013.

[6] J. Rios-Torres, P. Sauras-Perez, R. Alfaro, J. Taiber, and P. Pisu, "Eco-Driving System for Energy Efficient Driving of an Electric Bus," *SAE Int. J. Passeng. Cars Electron. Electr. Syst.*, 2015.

[7] J. Rios-Torres and A. A. Malikopoulos, "An overview of driver feedback systems for efficiency and safety," in *Proceedings of 2016 IEEE 19th International Conference on Intelligent Transportation Systems,*, 2016, pp. 667–674.

[8] B. Schrank, B. Eisele, T. Lomax, and J. Bak, "2015 Urban Mobility Scorecard," Texas A& M Transportation Institute, Tech. Rep., 2015.

[9] J. Rios-Torres and A. A. Malikopoulos, "A Survey on Coordination of Connected and Automated Vehicles at Intersections and Merging at Highway On-Ramps," *IEEE Transactions on Intelligent Transportation Systems*, vol. 18, no. 5, pp. 1066–1077, 2017.

[10] M. Athans, "A unified approach to the vehicle-merging problem," *Transportation Research*, vol. 3, no. 1, pp. 123–133, 1969.

[11] G. Schmidt and B. Posch, "A two-layer control scheme for merging of automated vehicles," in *The 22nd IEEE Conference on Decision and*

This article has been accepted for publication in a future issue of this journal, but has not been fully edited. Content may change prior to final publication. Citation information: DOI 10.1109/TIV.2018.2873899, IEEE Transactions on Intelligent Vehicles

*Control*, 1983, pp. 495–500.

[12] T. Awal, L. Kulik, and K. Ramamohanrao, "Optimal traffic merging strategy for communication- and sensor-enabled vehicles," in *Intelligent Transportation Systems - (ITSC), 2013 16th International IEEE Conference on*, 2013, pp. 1468–1474.

[13] J. Rios-Torres, A. A. Malikopoulos, and P. Pisu, "Online Optimal Control of Connected Vehicles for Efficient Traffic Flow at Merging Roads," in *2015 IEEE 18th International Conference on Intelligent Transportation Systems*, 2015, pp. 2432 – 2437.

[14] I. A. Ntousakis, I. K. Nikolos, and M. Papageorgiou, "Optimal vehicle trajectory planning in the context of cooperative merging on highways," *Transportation Research Part C: Emerging Technologies*, vol. 71, pp. 464–488, 2016.

[15] J. Rios-Torres and A. A. Malikopoulos, "Automated and Cooperative Vehicle Merging at Highway On-Ramps," *IEEE Transactions on Intelligent Transportation Systems*, vol. 18, no. 4, pp. 780–789, 2017.

[16] ——, "Energy impact of different penetrations of connected and automated vehicles," in *Proceedings of the 9th ACM SIGSPATIAL International Workshop on Computational Transportation Science - IWCTS '16*. ACM Press, 2016, pp. 1–6. [Online]. Available: http://dl.acm.org/citation.cfm?doid=3003965.3003969

[17] A. Mosebach, S. Röchner, and J. Lunze, "Merging control of cooperative vehicles," *IFAC-PapersOnLine*, vol. 49, no. 11, pp. 168–174, 2016. [Online]. Available: http://linkinghub.elsevier.com/retrieve/pii/S2405896316313477

[18] C. Letter and L. Elefteriadou, "Efficient control of fully automated connected vehicles at freeway merge segments," *Transportation Research Part C: Emerging Technologies*, vol. 80, pp. 190–205, jul 2017. [Online]. Available: http://linkinghub.elsevier.com/retrieve/pii/S0968090X17301274

[19] B. Ran, S. Leight, and B. Chang, "Microscopic Simulation Analysis for Automated Highway System Merging Process," *Transportation Research Record: Journal of the Transportation Research Board*, vol. 1651, pp. 98–106, jan 1998. [Online]. Available: http://trrjournalonline.trb.org/doi/10.3141/1651-14

[20] K. Li and P. Ioannou, "Modeling of Traffic Flow of Automated Vehicles," *IEEE Transactions on Intelligent Transportation Systems*, vol. 5, no. 2, pp. 99–113, jun 2004. [Online]. Available: http://ieeexplore.ieee.org/document/1303540/

[21] A. Talebpour and H. S. Mahmassani, "Influence of connected and autonomous vehicles on traffic flow stability and throughput," *Transportation Research Part C: Emerging Technologies*, vol. 71, pp. 143–163, oct 2016. [Online]. Available: http://linkinghub.elsevier.com/retrieve/pii/S0968090X16301140

[22] P. Gipps, "A behavioural car-following model for computer simulation," *Transportation Research Part B: Methodological*, vol. 15, no. 2, pp. 105–111, apr 1981. [Online]. Available: http://linkinghub.elsevier.com/retrieve/pii/0191261581900370

[23] U.S. Department of Transportation. Federal Highway Administration, "Traffic Analysis Toolbox Volume III: Guidelines for Applying Traffic Microsimulation Modeling Software," 2004. [Online]. Available: https://ops.fhwa.dot.gov/trafficanalysistools/tat_vol3/index.htm

[24] A. A. Malikopoulos, D. N. Assanis, and P. Y. Papalambros, "Optimal engine calibration for individual driving styles," in *SAE Proceedings, Technical Paper 2008-01-1367*, 2008.

[25] A. A. Malikopoulos, P. Y. Papalambros, and D. N. Assanis, "Online identification and stochastic control for autonomous internal combustion engines," *Journal of Dynamic Systems, Measurement, and Control*, vol. 132, no. 2, pp. 024 504–024 504, 2010.

[26] A. A. Malikopoulos, "A multiobjective optimization framework for online stochastic optimal control in hybrid electric vehicles," *IEEE Transactions on Control Systems Technology*, vol. 24, no. 2, pp. 440–450, 2016.

[27] A. A. Malikopoulos, C. G. Cassandras, and Y. Zhang, "A decentralized energy-optimal control framework for connected automated vehicles at signal-free intersections," *arXiv:1602.03786 - (in review)*, 2017.

[28] Y. Zhang, A. A. Malikopoulos, and C. G. Cassandras, "Optimal control and coordination of connected and automated vehicles at urban traffic intersections," in *Proceedings of the 2016 American Control Conference*, 2016, pp. 5014–5019.

[29] S. Panwai and H. Dia, "Comparative evaluation of microscopic car-following behavior," *IEEE Transactions in Intelligent Transportation Systems*, vol. 6, no. 3, pp. 314–325, 2005.

[30] B. Ciuffo, V. Punzo, and M. Montanino, "Thirty Years of Gipps' Car-Following Model," *Transportation Research Record: Journal of the Transportation Research Board*, vol. 2315, pp. 89–99, dec 2012. [Online]. Available: http://trrjournalonline.trb.org/doi/10.3141/2315-10

[31] L. Vasconcelos, L. Neto, S. Santos, A. B. Silva, and Á. Seco, "Calibration of the Gipps Car-following Model Using Trajectory Data," *Transportation Research Procedia*, vol. 3, pp. 952–961, 2014. [Online]. Available: http://linkinghub.elsevier.com/retrieve/pii/S2352146514002385

[32] M. A. S. Kamal, M. Mukai, J. Murata, and T. Kawabe, "Ecological Vehicle Control on Roads With Up-Down Slopes," *IEEE Transactions on Intelligent Transportation Systems*, vol. 12, no. 3, pp. 783–794, Sept. 2011.

**Jackeline Rios-Torres** (M2015) received her B.S. in electronic engineering from the Universidad del Valle, Colombia, in 2008 and the Ph.D. in Automotive Engineering from Clemson University in 2015. She is currently a Eugene P. Wigner Fellow with the Energy and Transportation Science Division at Oak Ridge National Laboratory. Her research is focused on connected and automated vehicles, intelligent transportation systems and modeling and energy management control of HEVs/PHEVs. Jackeline is a GATE fellow at the Center for Research and Education in Sustainable Vehicle Systems at CU-ICAR. She has also been a recipient of the Southern Automotive Women Forum scholarship and the Smith fellowship at CU-ICAR.

**Andreas A. Malikopoulos** (M2006, SM2017) received a Diploma in Mechanical Engineering from the National Technical University of Athens, Greece, in 2000. He received M.S. and Ph.D. degrees from the Department of Mechanical Engineering at the University of Michigan, Ann Arbor, Michigan, USA, in 2004 and 2008, respectively. He is an Associate Professor in the Department of Mechanical Engineering at the University of Delaware (UD) and an ASME Fellow. Before he joined UD, he was the Deputy Director and the Lead of the Sustainable Mobility Theme of the Urban Dynamics Institute at Oak Ridge National Laboratory, and a Senior Researcher with General Motors Global Research & Development. His research spans several fields, including analysis, optimization, and control of cyberphysical systems; decentralized systems; and stochastic scheduling and resource allocation problems. The emphasis is on applications related to sociotechnical systems, energy efficient mobility systems, and sustainable systems.